Table 2. Pb(0)-catalyzed coupling reaction of allyl *N*-acyl-*N*-tosylimide (**2b**, **2c**)

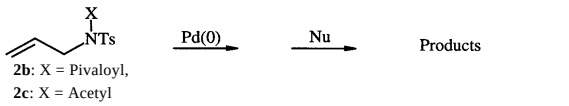

Entry	X	Nucleophile	Reaction condition	Products & yield (%)[a]
1	Pivaloyl	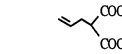	20°C, 3.5 h	(70) (7)
2	Pivaloyl	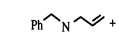	20°C, 4 h	(39) (14) (13)
3	Pivaloyl		20°C, 10 min	No rxn. 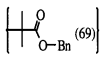 (69)
4	Pivaloyl	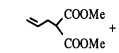	20°C, 11 h	(45) (2) (37)
5	Pivaloyl	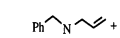	20°C, 11 h	(31) (14) (49)
6	Pivaloyl		20°C, 10 min	No rxn. 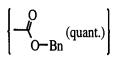 (quant.)

[a]All yields are isolated ones.

References

1. Current address: C&C Research Labs., Hwasung-goon, Kyunggi-do, 445-970, Korea.
2. (a) For an excellent review, see: Godleski, S. A. Nucleophiles with Allyl-Metal Complexes. In *Comprehensive Organic Synthesis*; Trost, B. M. Ed.; Pergamon: Oxford, 1991; Vol. 4, Chap. 3.3, pp 585-661. (b) Trost, B. M. *Angew. Chem., Int. Ed. Engl.* **1986**, *25*, 1. (c) Tsuji, J. *Tetrahedron* **1986**, *42*, 4361.
3. (a) Dzhemilev, U. M.; Minsker, D. L.; Khalilov, L. M.; Ibragimov, A. G. *Izv. Akad. Nauk SSSR, Ser. Khim. 1988*, 378. (b) Hosomi, A.; Hoashi, K.; Kohra, S.; Tominaga, Y.; Otaka, K.; Sakurai, H. *J. Chem. Soc., Chem. Commun*. **1987**, 570. (c) Hirao, T.; Yamada, N.; Ohshiro, Y.; Agawa, T. *Organomet. Chem.* **1982**, *236*, 409. (d) Tamura, R.; Hegedus, L. S. *J. Am. Chem. Soc*. **1982**, *104*, 3727. (e) Trost, B. M.; Keinan, E. *J. Org. Chem*. **1980**, *45*, 2741.
4. (a) Harris, G. D., Jr.; Herr, R. J.; Weinreb, S. M. *J. Org. Chem*. **1993**, *58*, 5452. (b) Jung, M. E.; Rhee, H. *J. Org. Chem*. **1994**, *59*, 4719. (c) Katagiri, N.; Masahiro, T.; Hideaki, K.; Chikara, K.; Kouichi, K.; Masahiro, T. *J. Org. Chem*. **1997**, *62*, 1580.
5. Hegedus, L. S. Palladium in Organic Synthesis. In *Organometallics in Synthesis*; Schlosser, M. Ed.; John Wiley & Sons, 1994; Chap. 5.4.3, pp 427-428.

Formation of Self-assembled Zirconium *N,N'*-Bis (benzyl phosphonic acid)-3,4,9,10-perylene(dicarboximide) Multilayer Films on Silicon Substrate

Hyun Jin Chae, Myung Soon Lee[†], Yeong Il Kim[†*], and Haiwon Lee[*]

Department of Chemistry, Hanyang University, Seoul 133-791, Korea
[†]Department of Chemistry, Pukyong National University, Pusan 608-737, Korea
Received September 18, 1997

Self-assembled mono- and multilayer formed on solid substrates have generated considerable interest because of the potential of controlling the molecular architecture and chemical and physical properties of layered assemblies on surfaces such as electron transfer, nonlinear optics, photocatalysis, molecular recognition. Researchers have utilized the transition metal phosphonates multilayer films on surfaces to study a system in which interlayer distance and orientation of the organic components are crucial. The metal phosphonate films provide an attractive means of constructing thermally and sovolytically stable films of controlled thickness, which consist of spatially well-defined molecular components[1-4]. In this communication, we report on the preparation of multilayer of zirconium *N,N'*-bis(benzyl phosphonic acid)-3,4,9,10-perylene(dicarboximide)(Zr-BPPI) based on the sequential adsorption of metal ion and bisphosphonic acid and on the characterization of the mutilayer structure using UV-visible absorption measurement, ellipsometry, and cyclic voltammetry. The perylenedicarboximide derivatives have been well known as photoconducting materials in xerography[5-7] and as photoinduced electron transporting materials. The photoconductivity of the BPPI comes from the strong π-π interactions between fused aromatic ring structures. One of the goals of our research is to incorporate photoactive BPPI molecules into multilayer assemblies, in order to prepare thin films which undergo efficient photoinduced chage separation and directional conductivity.

In the multilayer structure of Zr-BPPI presented here the adjacent perylene chromophore in each layer can be stacked each other perpendicularly to the substrate as shown sche-

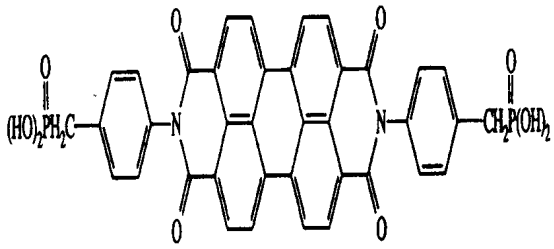

Figure 1. The structure of BPPI

matically in Figure 2. BPPI was prepared from the condensation reaction of 3,4,9,10-perylenedicarboxylic dianhydride and 4-amino benzyl phosphonic acid, which is preapared from acid hydrolysis of diethyl 4-aminobenzyl phosphonate, in a molten imidazol with zinc acetate at 170 °C BPPI was confirmed from IR absorption peaks[8]. The absorption peak, 1774 cm^{-1} of CO in dianhydride has been changed to 1701 and 1661 cm^{-1} of CO in imide. The BPPI is not soluble in any other solvents except in H_2O. But since the compound exists as a dimer due to the strong aromatic ring interaction, the NMR spectrum in D_2O was very broad and not discernible. Zr-BPPI films were grown using a methodology developed by Katz[9]. The cleaned silicon substrate was rinsed with acetonitrile and then phosphorylated by treatment with an acetonitrile solution of $POCl_3$ and 2,4,6,-collidine(10 mM in each) for 12h at 80 °C. The substrates were zirconated in a 5 mM solution of $ZrOCl_2$ for 3h at room temperature. Multilayers of Zr-BPPI were produced by alternate dippings in 5 mM BPPI and $ZrOCl_2$ solution at room temperature for 1 h. Films were thoroughly rinsed with deionized water between dippings.

The UV spectra of Zr-BPPI multilayer films on quartz plate displayed a strong absorbance at 500 nm and 542 nm and those of BPPI solution exhibits a strong absorption band at 508 nm. This results indicates that the Zr-BPPI films is grown uniformly by the effective π-π interactions among inter- and intramolecules. Figure 3 shows the UV absorbance at 500 nm as a function of the number of layer of Zr-BPPI films on a quartz plate.

As the number of layer increased, the absorbance of the film increased linearly. Figure 4 shows the thickness of BPPI multilayer films as a function of the number of layer. Under the assumption that the Zr-BPPI layer has the same refractive index of Zr-decanebisphosphonate layer[3], the average

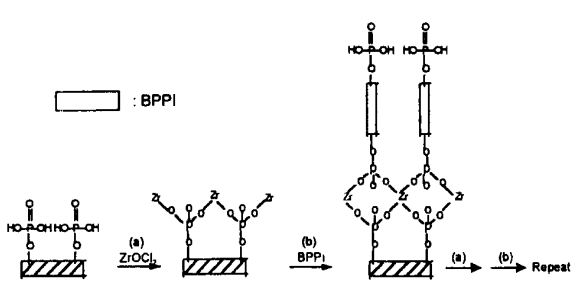

Figure 2. Synthetic scheme for the formation of Zr-BPPI multilayers.

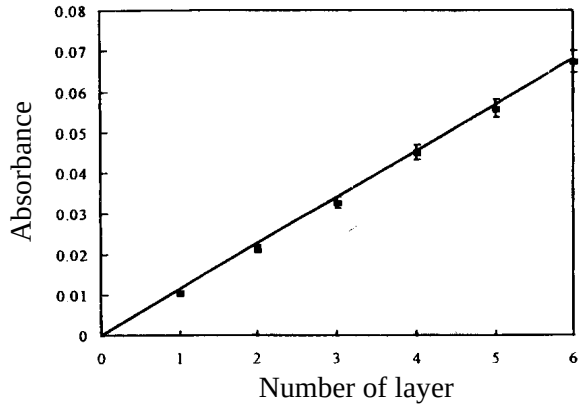

Figure 3. Measured UV-vis absorbance at 500 nm as a function of the number of layer of Zr-BPPI deposited on a quartz plate.

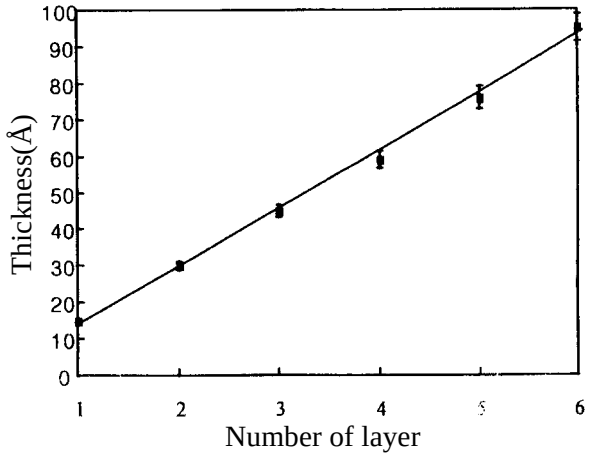

Figure 4. Thickness of Zr-BPPI multilayer films as a function of the number of layer calculated from ellipsometry data.

thickness of layer was determined. In the plot of the number of layer vs thickness, the slope of the line related to the average thickness of layer is 15.8 Å/layer. The straight-line indicates that individual layer is uniformly grown in average thickness[10].

The mulilayers of Zr-BPPI can be grown on the nanoporous particulate films as well as planar substrates such as silicon and quartz. Figure 5 shows cyclic voltammograms of BPPI layers on nanoporous TiO_2 film electrode.[11] The quasi-reversible peak currents are systematically increased as the number of layer increases although the cathodic peaks are higher than anodic ones. The reason for the difference is not clear at this point. Control experiments showed that the redox peak currents do not increase without treatment of zirconyl chloride solution in each layer-growing step. As the layers grow, the integrated charges of cathodic peaks after background substraction are almost linearly increased (not shown here).

It shows that the adsorbate concentration in each layer is pretty constant. Since the absorption spectrum of BPPI is different from the reduced BPPI, we are currently investigating the possibility of electrochromic device using these

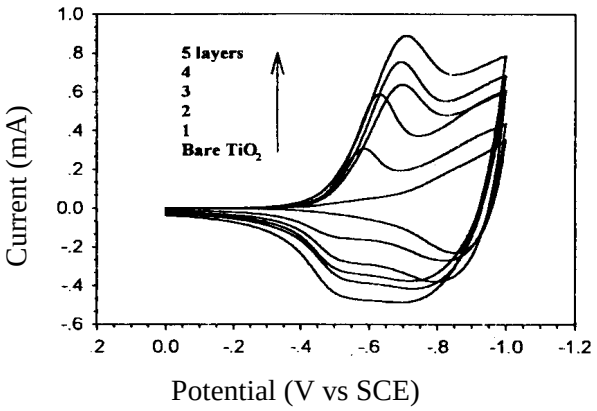

Figure 5. Cyclic voltammogram of BPPI layer on TiO_2.

redox couple multilayer. Although UV spectra, ellipsometric measurements, and cyclic voltammogram suggest that the Zr-BPPI films grow uniformly, the atomic images of multilayer films are needed to confirm the uniformity of films. Therefore, the AFM measurement of Zr-BPPI films is being carried out to study film uniformity and growth on a microscopic level.

In summary, it is shown that the layer thickness measured by ellipsometry linearly increases as a function of the number of layer deposited and UV-vis spectroscopic results of the deposition process are consistent with those of ellipsometric measurements. The average thickness of the film derived by ellipsometry was observed about 15.8 Å. Also, according to cyclic voltamogram, the quasi-reversible peak currents are systematically increased as the number of layer increases. These results indicate that the same amount of BPPI layer is placed on the substrate after each deposition cycle.

Acknowledgment. This work was supported by the Ministry of Education (BSRI-96-3427)

References

1. Dines, M. B.; Griffith, P. C. *Inorg. Chem.* **1983**, *22*, 567.
2. Zeppenfeld, A. C.; Fiddler, S. L.; Ham, W. K.; Klopfenstein, B. J.; Page, C. J. *J. Am. Chem. Soc.* **1994**, *116*, 9158.
3. (a) Lee, H.; Kepley, L. J.; Hong, H. G.; Mallouk, T. E. *J. Am. Chem. Soc*. **1988**, *110*, 618. (b) Akhter, S.; Lee, H.; Hong, H. G.; Mallouk, T. E.; White, J. M. J. *J. Vac. Sci. Technol.* **1989**, *7*, 1608.
4. Vermeulen, L. A.; Snover, J. L.; Sapochak, L. S.; Thomson, M. E. *J. Am. Chem. Soc*. **1993**, *115*, 11767.
5. Law, K. Y. *Chem. Rev.* **1993**, *93*, 449.
6. Heribert, Q.; Yves, G.; Klaus, M. *Chem. Mater*. **1997**, *9*, 495.
7. Halls, J. J. M.; Friend, R. H. *Synthetic Metals*. **1997**, *85*, 1307.
8. Langhals, H. *Chem. Ber*. **1985**, *118*, 4641.
9. (a) Putvinski, T. M.; Schilling, M. L.; Katz, H. E. *Langmuir*. **1990**, *6*, 1567. (b) Katz, H. E.; Wilson, W. L.; Scheller, G. *J. Am. Chem. Soc*. **1994**, *116*, 6636. (c) Katz, H. E.; Scheller, G.; Putvinski, T. M.; Schilling, M. L.; Wilson, W. L.; Chidsey, C. E. D. *Science.* **1991**, *254*, 1485.
10. Snover, J. L.; Byrd, H.; Suponeva, E. P.; Vicenzi, E.; Thomson, M. E. *Chem. Mater*. **1996**, *8*, 1490.
11. Nanoporous TiO_2 film electrode was prepared using Degussa P25 TiO_2 by the method of Graetzel et al's[12]. The thickness of the TiO_2 film is about 4 μm estimated from SEM picture. The geometric area of the electrode is 1.5 cm^2. However the actual surface area of the TiO_2 electrode is about 1000 times higher than that considering nanoporous nature. The cyclic voltammograms were measured in three cell electrode system with Pt counter and SCE reference electrode. The electrolyte solution was 0.1 M KCl and the scan rate was 25 mV/sec. The detail electrochemical studies of these multilayers on the TiO_2 electrode will be presented in the other paper.
12. Nazeerudin, M. K.; Rodicio, I. R.; Baker, H.;Liska, P.;Vlachopoulos, N.; Grizel, M. *J. Am. Chem. Soc.* **1993**, *115*, 6382.

Kinetic Analysis of Inactivation of the cdc25 Phosphatase by Menadione

Seung Wook Ham*, Ji Sang Yoo, Junguk Park, and Hyeongjin Cho†

Department of Chemistry, Chung-Ang University, Seoul 156-756, Korea
†Department of Chemistry, Inha University, Inchon 402-751, Korea
Received September 26, 1997

Cdc25 phosphatases catalyze tyrosine-15 dephosphorylation of the $p34^{cdc2}$, catalytic subunit of the M phase-Promoting Factor (MPF);[1,2] this leads to the G2/M transition of the cell cycle in all organisms.[3,4] These enzymes play an important role in the regulation of cell division cycle and present a promising target for the design of potential chemotherapeutic agents in the field of antitumor treatment.[5~7]

Since it has been reported that menadione induced alterations in the phosphorylation status and the activity of protein tyrosine phosphatase,[8] and menadione shares a enone structure with some mechanism-based inhibitors of phosphatases that have been previously reported,[9,10] we have re